

# Mechanical Analysis of Yang chaotic System and its Synchronization

Dr. Amrita Singh

Department of Mathematics, MRM College, Darbhanga, India.

Abstract: This study presents a mechanical analysis of the Yang chaotic system by transforming it into a Kolmogorov-type system, decomposed into four torque components: inertial, internal, dissipative, and external. Five scenarios, involving various torque combinations, are explored to identify the key element of chaos and their physical implications. The conversion between Hamiltonian, potential, and kinetic energy is investigated in these five situations. The interplay between the energy and the parameters is investigated. The study concludes that in order to create chaos in a Yang chaotic system, a combination of these four types of torques is required, since any combination of the three types of torques cannot. Furthermore, identical Yang chaotic systems are synchronized by function matrix projective synchronization (FMPS).

**Keywords:** Yang chaotic system, mechanical analysis, chaotic system, matrix projective synchronization and dissipative systems.

1. Introduction: The last several decades have seen a major impact on nonlinear dynamics in the field of science and engineering. The dynamical system is employed to investigate how natural occurrences evolve. From an application perspective, the dynamical systems that are highly sensitive to initial conditions can be effectively exploited for secure communications [1]. Numerous scientific disciplines have identified chaos, which is prevalent in nature. Lorenz [2] discovered the first chaotic attractor in 1963. It is a pioneering illustration of deterministic chaos in dissipative systems. Another similar chaotic attractor, dual to the Lorenz system but not topologically identical to the Lorenz chaotic attractor, was found by Chen and Ueta [3] in 1999.

Researchers are motivated to study chaotic systems by the applicability aspect. Numerous fields, including physics, biology, and secure communication, have found use for it. Chaotic systems were first used in communication by Pecora and Carrol [4, 5]. The complex dynamical system becomes a herculean task for the engineers and scientists working in the field of mathematical modeling.

Over the past few decades, experts from all over the world have examined the effect of chaos in nonlinear dynamical systems and various physical chaotic systems exhibit this effect most frequently. For application point of view, chaos frequently limits the operational range of mechanical and electrical systems, making it an undesirable phenomenon.

Generally, the closed-form analytical solutions are not possible due to the intricacy of the dynamical systems. Therefore, the qualitative behavior of an equilibrium point of a dynamical system must be determined using the alternative way of analysis. There are a few chaotic systems that are created by numerical simulation. The study of the chaotic systems must include system control, synchronization, and sensitivity to initiation, bifurcation theory, and numerical computation. The force analysis and mechanics of chaos for dynamical systems have attracted the attention of the researchers in the society of engineering.

However, very few scholars have studied the mechanics and physical underpinnings of chaos [6-10]. Therefore, locating the relevant terms in these numerically chaotic systems is an intriguing and difficult challenge. Mechanics examines the dynamics of particles, rigid bodies, and continuous media [11-15], explores the transformation of many types of energy and forces, and clarifies the meanings of physical concepts.

A combined analysis of the Kolmogorov and Lorenz systems was examined by Pelion and Pasini [16]. Qi and Liang [17] have investigated the mechanical analysis of the Qi four-wing chaotic system. They have identified the angular momentum, which is analogous to the state variable of the chaotic system. In order to describe hydrodynamic instability or dissipative-forced dynamical systems with a Hamiltonian function, Arnold [18] created a Kolmogorov system. They also used the extended Kolmogorov system to study the energy cycle of the Lorenz system. The Chen system was mechanically analyzed by Liang and Qi [19]. The Hamiltonian function and Kolmogorov system play a crucial role in investigating the mechanics of chaos. The 4D hyper chaotic system has been investigated by Benkouider et al. [20] within the framework of the Kolmogorov system.

In this exploration, we introduce a range of dynamic modes by blending different torques, delving into their energetic and dynamic properties to uncover how these forces contribute to the emergence of chaos. Our study sheds light on the physical implications of diverse mechanical modes. The primary aim is to examine the forces that spark chaotic behavior. Chaotic systems are marked by two key traits: sensitivity to initial conditions and bounded solutions. A positive Lyapunov exponent suggests that, in non-chaotic systems, solutions expand without limits. In contrast, for a confined chaotic attractor, it reveals a trajectory that continuously stretches and folds within set boundaries.

Constructing suitable functions that are recognized as controllers to guarantee synchronization is one of the most important aspects to analyze dynamical systems. In order to comprehend the unique synchronization behavior of these systems, numerous mathematical models have been proposed [21-22]. Synchronization between master and slave systems in complex dynamical systems can be achieved with a scaling factor through projective synchronization. A variety of synchronization types, including as projective synchronization, anti-synchronization, and complete synchronization, be a particular case of function projective synchronization. Depending on the scale function matrix, specific synchronization outcomes are possible: a constant matrix produces matrix projective synchronization (MPS). The MPS offers a wider range of applications than traditional projective synchronization, especially in enhancing message security. Due to its increased complexity relative to other synchronization methods in chaotic systems, MPS is a critical approach for synchronizing intricate, multidimensional, or highly interactive systems. MPS is more complex than other synchronization forms in chaotic systems, making it a crucial approach for synchronizing complex systems, particularly in multidimensional or intricately interacting systems.

(1)

FMPS enables the slave system to be directed by the master system through an arbitrary matrix, thereby strengthening communication security via enhanced chaotic masking. Ouannas and Abu-Saris [23] established new controller, defining essential conditions and criteria for synchronization. The FMPS has also been explored by multiple scholars [24-26]. Additionally, FMPS approach bolsters security by incorporating unpredictability into the scale function matrix, attracting significant interest from the research community [27-29]. Motivated by this growing interest, the authors examine the FMPS of the Yang chaotic system.

This article organizes the remaining sections as follows: Section 2 incorporates the mathematical equations of the Yang system and its mechanical decomposition in Kolmogorov formalism. Section 3 examines the mechanisms underlying various modes of Yang chaotic attractor. Section 4 explores the FMPS of Yang chaotic system. Section 5 provides a concise conclusion.

## 2. System's Description

The Yang chaotic system in [30] is described as

$$\dot{\xi_1} = \alpha \left( \xi_2 - \xi_1 \right)$$

$$\dot{\xi_2} = -\xi_1 \, \xi_3 + \gamma \xi_1$$

$$\dot{\xi_3} = \xi_1 \xi_2 - \beta \xi_3$$

where  $\alpha$ ,  $\beta$  and  $\gamma$  be the parameters.

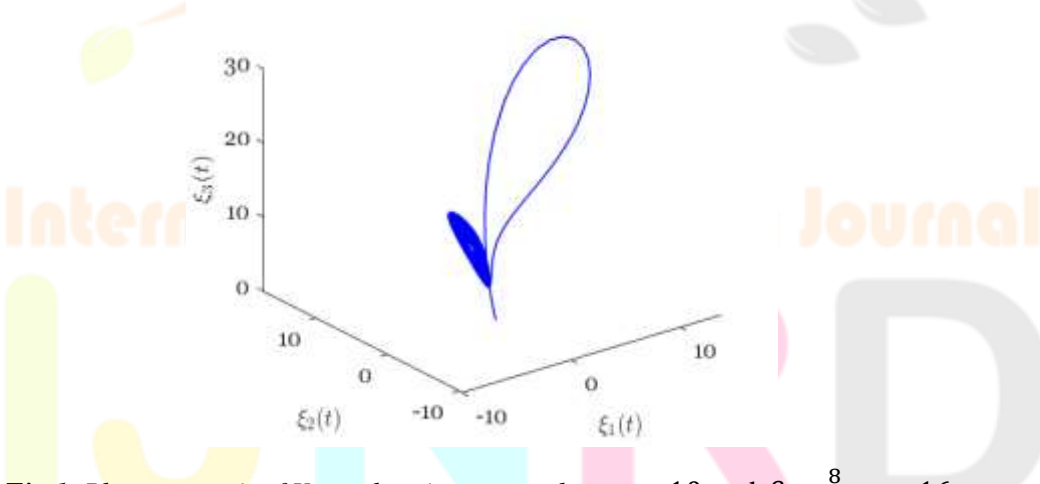


**Fig 1.** Phase portrait of Yang chaotic system when  $\alpha = 10$  and  $\beta = \frac{8}{3}$ ,  $\gamma = 16$ .

Now apply a linear transformation  $\xi_1 = \xi_1$ ,  $\xi_2 = \xi_2$ ,  $\xi_3 = \xi_3 - \gamma$ , further the system is given by

$$\dot{\xi_1} = \alpha \left( \xi_2 - \xi_1 \right)$$

$$\dot{\xi}_2 = 2\gamma \xi_1 - \xi_1 \xi_3 \tag{2}$$

$$\dot{\xi}_3 = \xi_1 \xi_2 - \beta \xi_3 + \beta \gamma$$

We provide the Euler equation and the Kolmogorov system to determine the physical equivalent of the system's state variables and mechanics. Arnold's Kolmogorov system, which simulates hydrodynamic instabilities [18] was previously characterized in three dimensions as

$$\dot{\xi} = \{\xi, H\} - \Lambda \, \xi + \psi \tag{3}$$

The anti-symmetric brackets  $\{.,.\}$  represent the algebraic structure associated with the Hamiltonian function, indicating the presence of centrifugal and internal force components [19]. The system's dissipation is represented by the positive definite diagonal matrix  $\Lambda \xi$ . The magnitude of the external force field is indicated by  $\psi$ .

The Lie-Poissions bracket is given by

$$\{E, P\}(\xi) = -\xi. (\nabla E \times \nabla P) = -\varepsilon_{jk}^{i} x_{i} \frac{\partial P}{\partial x_{i}} \frac{\partial P}{\partial x_{k}}; \quad i, j, k = 1, 2, 3.$$

$$(4)$$

where  $E, P \in C^{\infty}(g^*)$ , g represents Lie-algebra and  $\varepsilon_{jk}^i$  represents Levi-Civita tensor. System (3) is introduced by Kolmogorov to identify the instability of hydrodynamic systems as reported by Arnold [18] in 1991.

By defining the Hamiltonian as H = K + U, where  $K = (\xi_1^2 + \xi_2^2 + \xi_3^2)/2$ ,  $U = (\alpha + 2\gamma)\xi_3$  represents kinetic and potential energy respectively. The Yang chaotic system (2) is characterized as a Kolmogorov-type system,

$$\dot{\xi} = \begin{pmatrix} \alpha \xi_2 \\ 2\gamma \xi_1 - \xi_1 \xi_3 \\ \xi_1 \xi_2 \end{pmatrix} - \begin{pmatrix} \alpha \xi_1 \\ 0 \\ \beta \xi_3 \end{pmatrix} + \begin{pmatrix} 0 \\ 0 \\ \beta \gamma \end{pmatrix}$$

$$= \{\xi, H\} - \Lambda \xi + \psi \tag{5}$$

where  $\xi = [\xi_1, \xi_2, \xi_3]^T$ ,  $\Lambda = diag\{\alpha, 0, \beta\}$  and  $\psi = (0, 0, \beta\gamma)^T$ .

System (3)'s first term,  $\{\xi, H\}$  is conservative by nature and includes internal torque and centrifugal forces that are derived from kinetic and potential energy respectively. Here, the time derivative  $\dot{\xi}$  represents the system's reaction torque, while the variable  $\xi$  represents the angular momentum.

#### 3. Mechanical Analysis

In order to determine the critical factor that causes chaos, this section looks at the dynamic modes of the chaotic system (5), which correlate to various types of torque. On the other hand, energy is easier to understand because it is a scalar quantity.

Case 1: System under inertial torque:

The equivalent mechanical equation is given as

$$\dot{\xi} = \{\xi, K\} = \begin{pmatrix} 0 \\ -\xi_1 \xi_3 \\ \xi_1 \xi_2 \end{pmatrix} \tag{6}$$

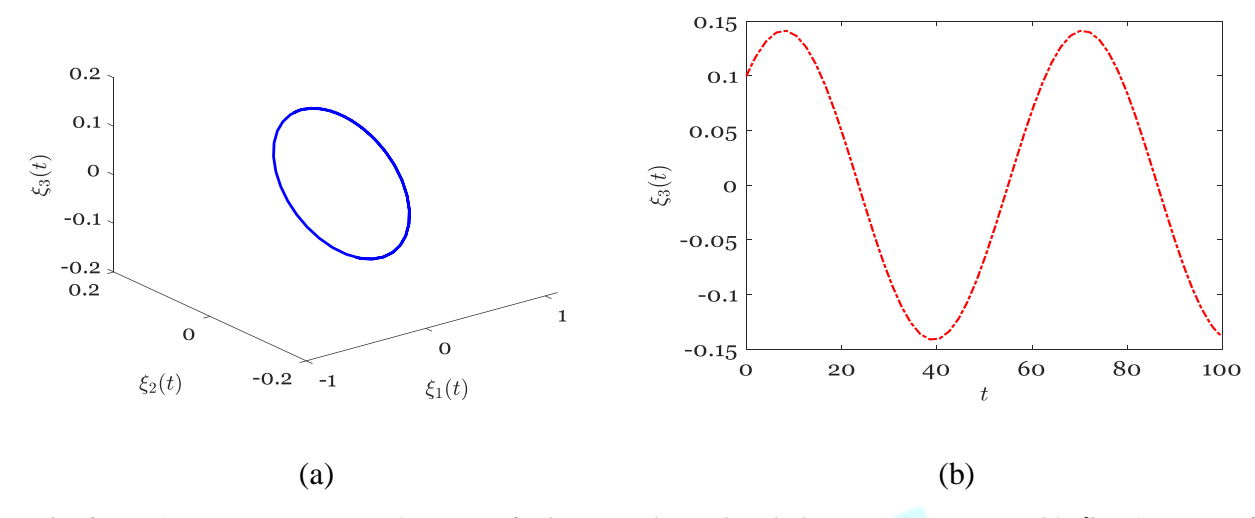


**Fig. 2.** (a) 3D representation of system (6) (b) Time dependent behavior of state variable  $\xi_3$  of system (6).

The time derivative of kinetic energy is  $\dot{K} = \xi_1 \dot{\xi}_1 + \xi_2 \dot{\xi}_2 + \xi_3 \dot{\xi}_3 = 0$ . Consequently, a conservative approach is taken by the system (6) subjected to kinetic energy. The graphical representation of conservative nature of the system (6) is demonstrated through Fig. 2 (a) while state variable of  $\xi_3$  is represented by Fig. 2 (b).

## Case 2: System under internal and inertial torque:

The corresponding mechanical equation is given as

$$\dot{\xi} = \{\xi, H\} = \{\xi, K\} + \{\xi, U\} = \begin{pmatrix} \alpha \xi_2 \\ 2 \gamma \xi_1 - \xi_1 \xi_3 \\ \xi_1 \xi_2 \end{pmatrix}. \tag{7}$$

Fig. 3. (a) Three-Dimensional Visualization of Periodic Trajectories; (b) Time dependent representation of state variable  $\eta_3$ . The derivative of Hamiltonian function is  $\dot{H} = \xi_1 \dot{\xi}_1 + \xi_2 \dot{\xi}_2 + \xi_3 \dot{\xi}_3 + (2\gamma + \alpha) \dot{\xi}_3 = 0$ . Therefore, Hamiltonian is constant i.e. conservation of energy holds. Subsequently, a closed periodic orbit is demonstrated through Fig. 3(a) while the state variable  $\xi_3$  is illustrated through Fig. 3(b). Additionally, all the Lyapunov exponent vanishes and Lyapunov dimension  $(L_d)$  is 3. Therefore, the conservation of system (7) is confirmed.

#### Case 3: System subjected to inertial, internal and dissipative torques:

The corresponding mechanical equation is

$$\dot{\xi} = \{\xi, H\} - \Lambda \xi = \begin{pmatrix} \alpha \xi_2 \\ 2\gamma \xi_1 - \xi_1 \xi_3 \\ \xi_1 \xi_2 \end{pmatrix} - \begin{pmatrix} \alpha \xi_1 \\ 0 \\ \beta \xi_3 \end{pmatrix}$$
 (8)

when  $\alpha = 10$ , and  $\beta = \frac{8}{3}$ ,  $\gamma = 16$ , It is obtained as  $Div(V) = -(\alpha + \beta) < 0$  and V stands for the system's phase space volume. Due to exponential contraction of the volume,  $(t) = V(0)e^{-(\beta + \alpha)t}$ , system (8) must be dissipative. For Hamiltonian, the time derivative is given as

$$\dot{H} = -\alpha \xi_1^2 - \beta \xi_3^2 + \beta \gamma \xi_3,$$

Unlike the Kolmogorov system [19-20], we have not yet succeeded in determining the energy dissipation via the derivative of the Hamiltonian. Therefore, in order to characterize the dissipative behavior of system (8) the Casimir energy function [9] has been incorporated.

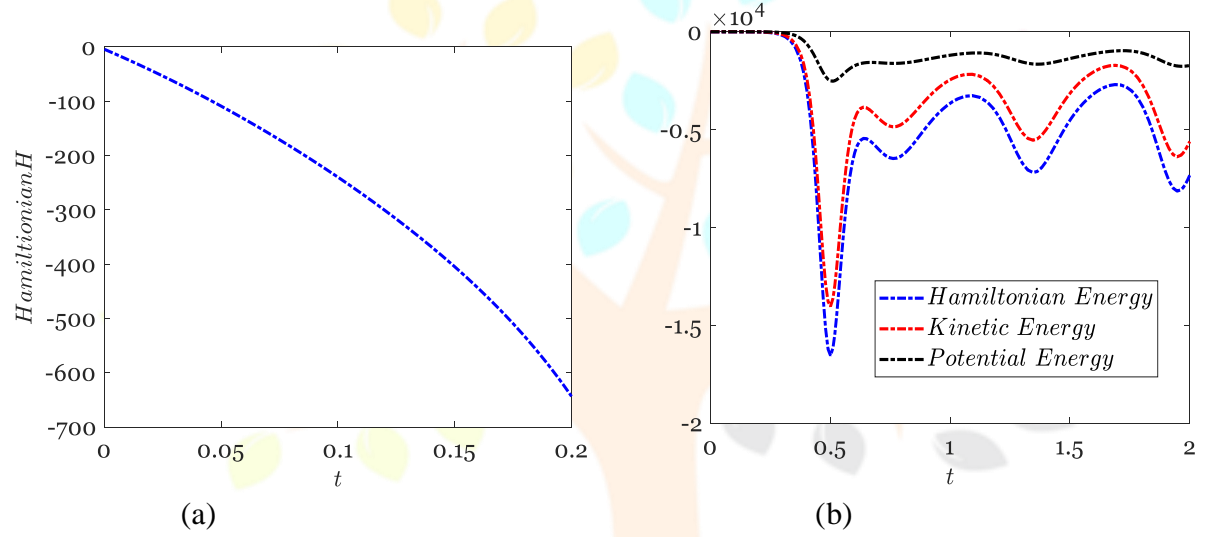


Fig. 4. (a) Variation of Hamiltonian energy with time, (b) Time-dependent behavior of energy functions.

The rate of change of Casimir energy can be expressed as

$$\dot{C} = \frac{\partial C}{\partial \eta} \dot{\eta}$$

$$= -(\xi_1^2 + \beta \xi_2^2) < 0$$

The system exhibits clear dissipative behavior. Figures 4(a) and 4(b) depict the Hamiltonian energy and energy functions, respectively, and demonstrate how the dissipative term causes the Hamiltonian energy to drop off significantly following the energy exchange. Therefore, Hamiltonian energy increases with time due to increase in kinetic energy as illustrated in the Fig.4 (b). The system is not conservative, as indicated by the variance in Hamiltonian energy, yet it is not chaotic because the Lyapunov dimension ( $L_d$ ) is 3, which is not fractal.

**Case 4:** when system subjected to inertial, internal and external torques:

The corresponding mechanical equation can be expressed as,

$$\dot{\xi} = \{\xi, H\} + \psi = \dot{\xi} = \begin{pmatrix} \alpha \xi_2 \\ 2\gamma \xi_1 - \xi_1 \xi_3 \\ \xi_1 \xi_2 \end{pmatrix} + \begin{pmatrix} 0 \\ 0 \\ \beta \gamma \end{pmatrix} \tag{9}$$

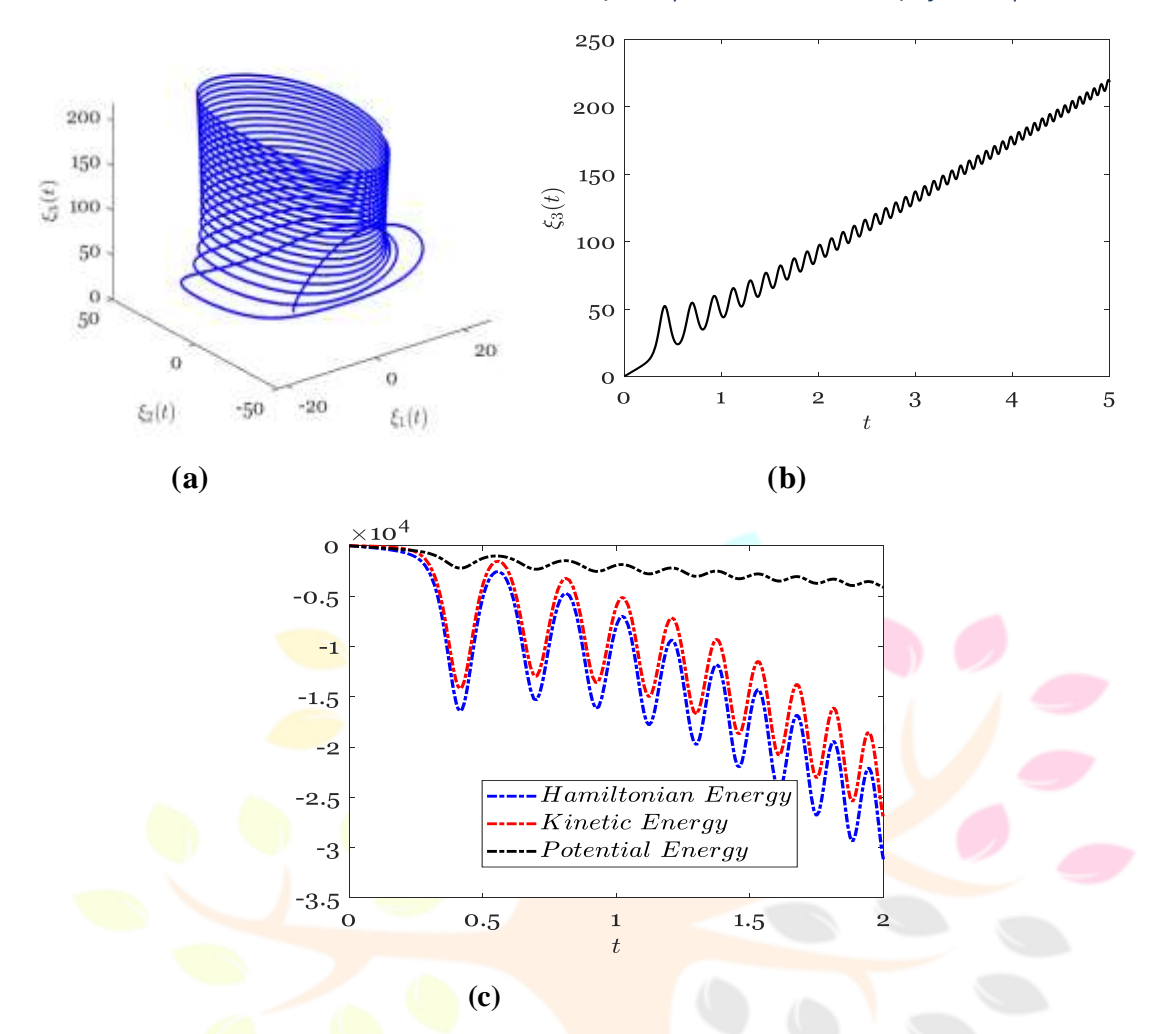


Fig. 5. (a) Three-Dimensional Visualization of Trajectories of system (9) (b) Time dependent behaviour of state variable  $\xi_3$  (c) Variation of energy functions with time.

As seen in Fig. 5(a), the external torque  $\psi$  causes the orbit to extend out into spiral-like arcs as a torus in addition to doubling its period. Fig. 5(b) depicts how state variables' oscillation frequencies increase fast with time.

Let 
$$V_1(t) = \frac{\xi_1^2}{2} - \alpha \xi_3$$
;  
then  $\dot{V}_1(t) = -\alpha \beta \gamma < 0$  and  $V_1(t) - V_1(0) = \int_0^t -2\alpha \gamma ds = -\alpha \beta \gamma t$ ;  
 $V_1(t) \to -\infty$  when  $t \to \infty$ .

That is, the state  $\xi_1$  or  $\xi_3$  is unbounded, as shown in Fig. 5(a). Therefore, the system is not chaotic. System (9) does not contains dissipative term and the energy contained in the system (9) as a result of external torque primarily enhances the kinetic energy. Therefore, Hamiltonian energy increases with time due to increase in kinetic energy as illustrated in the Fig.5 (c). Energy production and dissipation are prerequisites for a dissipative chaotic system.

**Case 5:** when system is under full torque:

$$\dot{\xi} = \begin{pmatrix} \alpha \xi_2 \\ 2\gamma \xi_1 - \xi_1 \xi_3 \\ \xi_1 \xi_2 \end{pmatrix} - \begin{pmatrix} \alpha \xi_1 \\ 0 \\ \beta \xi_3 \end{pmatrix} + \begin{pmatrix} 0 \\ 0 \\ \beta \gamma \end{pmatrix} = \{\xi, H\} - \wedge \xi + \psi$$
 (10)

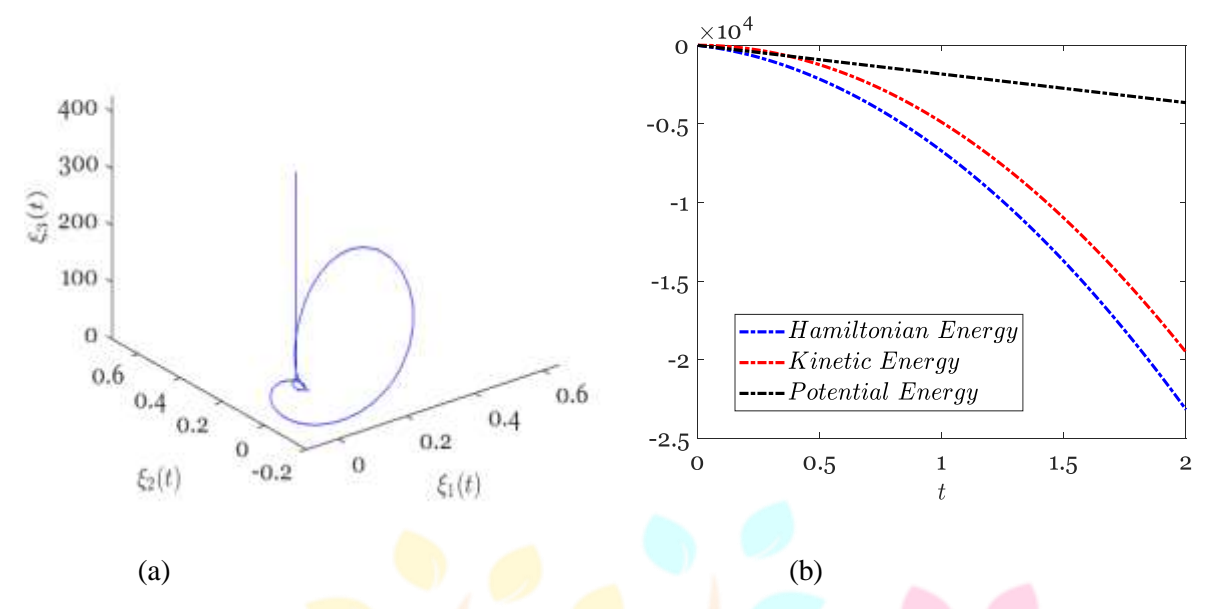


Fig.6. (a) Three-Dimensional Visualization of Trajectories of system (10) (b) Variation of energy functions with time.

It is evident that inertial torque and dissipation are required for chaos, but they are not enough on their own to cause chaotic behavior, as illustrated in case 3, where both elements are present yet chaos does not develop. Both internal and external torques are important drivers of chaotic dynamics in many systems. The chaotic system's orbit travels across a nearly two-dimensional curved surface, forming a chaotic attractor whose volume progressively compresses toward zero (Fig. 6(a)). The Fig. 6(b) demonstrates the relationship between kinetic and potential energy over time. The center curve shows the Hamiltonian energy, the bottom curve shows potential energy, and the upper curve shows kinetic energy. Nonetheless, the variation in Hamiltonian energy reveals the chaotic character of the system's energy behavior and points to a violation of conservation.

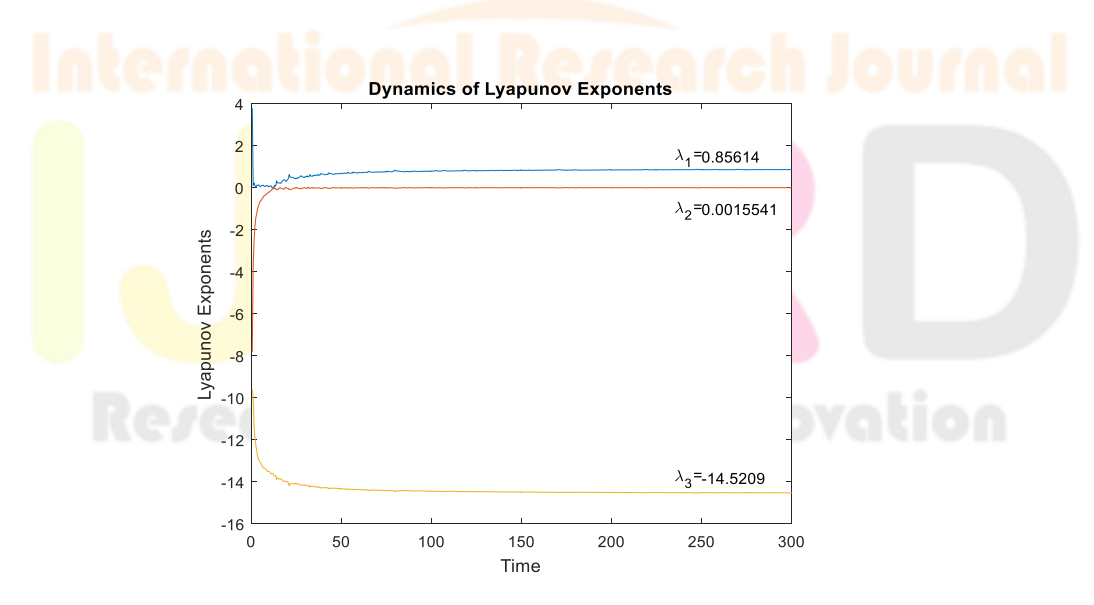


Fig.7. Dynamics of Lyapunov exponents of Yang system

Evidently, Lyapunov exponents for system (10) are  $L_1 = 0.85614$ ,  $L_2 = 0.00155$ ,  $L_3 = -14.5209$ , and Lyapunov dimension  $L_d = 2.05906$ . The chaotic characteristic of the Yang system is reflected in the fractal Lyapunov dimension for system (10).

### 4. Function matrix projective synchronization (FMPS):

Consider the following two non-identical chaotic systems:

$$\dot{\zeta}(t) = M\zeta + F(\zeta(t)), \tag{11} \quad \dot{\eta}(t) = N\eta + G(\eta(t)) + U,$$

(12) where  $\zeta(t) = (\zeta_1(t), \zeta_2(t), \zeta_3(t), ..., \zeta_m(t))^T, \eta(t) = (\eta_1(t), \eta_2(t), \eta_3(t), ..., \eta_m(t))^T \in \mathbb{R}^m, M \text{ and } N \text{ are } (12)^T \in \mathbb{R}^m$ 

 $n \times n$  matrices with nonlinearities F and G. The control parameter is U.

**Definition 4.1:** The master system (11) and slave system (12) are said to achieve function matrix projective synchronized (FMPS) if there exist a control function  $U(\zeta, \eta) \in R^m$  which satisfies  $\lim_{t \to \infty} \|\zeta - \chi \eta\| = 0$ ,

(13) where the constant matrix  $\chi$  is projective

matrix.

**Theorem 4.1:** Synchronization in the form of a functional matrix projection is attained between the master and slave systems (11) and (12), respectively, if there exists a controller  $U(\zeta, \eta) \in R^m$  such that

$$U = \chi [M\zeta + F(\zeta)] - G(\eta) - (N + \mu)\chi\zeta + \mu\eta$$
  
(N + \mu)<sup>T</sup> + (N + \mu) is negative definite.

(14) Provided

**Proof:** The error system associated with matrix projective synchronization has the following time derivative:

$$\dot{e} = \zeta - \chi \dot{\eta} - \dot{\chi} \eta .$$

The above equation together with (14) yields

$$\dot{e} = N\zeta + G(\zeta(t)) + U - \chi [M\eta + F(\eta(t))] - \dot{\chi}\eta$$
$$= (B + \mu)e$$

In order to analyze the stability of the error system, we define a Lyapunov-type function  $V = e^{T}e^{T}$  V, whose time derivative is expressed as,

$$\dot{V} = \dot{e}^T e + e^T \dot{e},$$

$$= e^T \left[ (N + \mu)^T + (N + \mu) \right] e < 0.$$

The condition derived above is satisfied when the matrix  $(N + \mu)^T + (N + \mu)$  is negative definite.

# 4.1 Matrix projective Synchronization (MPS):

The Yang chaotic system [30] is considered as master system

$$\dot{\xi_1} = \alpha \left( \xi_2 - \xi_1 \right)$$

$$\dot{\xi}_2 = -\xi_1 \, \xi_3 + \gamma \, \xi_1 \tag{15}$$

$$\dot{\xi}_3 = \xi_1 \xi_2 - \beta \xi_3$$

Further, the controlled slave system is supposed as

$$\eta_1 = \alpha(\eta_2 - \eta_1) + U_1 
\eta_2 = -\eta_1 \eta_3 + \gamma \eta_1 + U_2$$
(16)

$$\dot{\eta_3}=\eta_1\eta_2-\beta\eta_3+U_3$$

The function  $(U_1, U_2, U_3)^T$  serves as a control input intended to direct the behavior of slave system.

The projective matrix  $\varepsilon$  has been considered, to synchronize master system (15) and slave system (16), as

$$\chi = \begin{pmatrix} -1 & 0 & -1 \\ 1 & 1 & 0 \\ 0 & 1 & 2 \end{pmatrix}. \tag{17}$$
 The linear part

of response system yields

$$B = \begin{pmatrix} -\alpha & \alpha & 0 \\ \gamma & 0 & 0 \\ 0 & 0 & -\beta \end{pmatrix}.$$

(18) There are a

number choices for the gain matrix. In this case, the gain matrix has been regarded as  $\mu = \begin{pmatrix} 0 & -\alpha & 0 \\ -\gamma & -1 & 0 \\ 0 & 0 & 0 \end{pmatrix}$ .

(19) Finally, the equation (18) and (19) yields

$$B + \mu = \begin{pmatrix} -\alpha & 0 & 0 \\ 0 & -1 & 0 \\ 0 & 0 & -\beta \end{pmatrix}.$$

Now, equation (19) yields the control function as

$$\begin{split} &U_{1} = -\alpha(\eta_{2} - \eta_{1}) + \beta \eta_{3} - \eta_{1}\eta_{2} - \xi_{3} + \gamma - \alpha(\eta_{1} - \eta_{3}) - \alpha \xi_{2}, \\ &U_{2} = \alpha(\eta_{2} - \eta_{1}) - \eta_{1}\eta_{3} + \gamma \eta_{1} + \xi_{1}\xi_{3} + (\eta_{1} + \eta_{2}) - \gamma \xi_{1} - \xi_{2}, \\ &U_{3} = -\eta_{1}\eta_{3} + \gamma \eta_{1} + 2(\eta_{1}\eta_{2} - \beta \eta_{3}) - \xi_{1}\xi_{2} + \beta(\eta_{2} + 2\eta_{3}). \end{split}$$

Substituting the control function and the parameter values from equations (17), (18), and (19) into the control law, we obtain the error system as

$$\dot{e}_1 = -\alpha e_1, \dot{e}_2 = -e_2, \dot{e}_3 = -\beta e_3.$$
 (20) All of the

eigenvalues in the error system are negative, ensuring asymptotic stability. Consequently, the FMPS has been achieved in accordance with theorem 4.1.

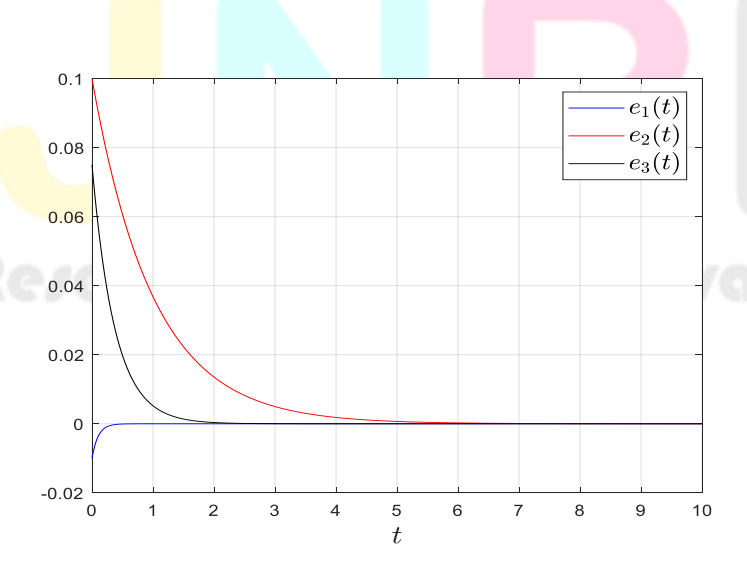


Fig.8. State trajectories of the error system over time

The IC (0.1, 0.1, 0.1) has been taken for Yong chaotic system, when a = 10,  $b = \frac{8}{3}$  and c = 16, the phase portrait of chaotic system in 3D space is illustrated through Fig.1. The Fig.8 reveals that the state trajectories of drive and response systems converges to zero, this authenticates the matrix projective synchronization has been achieved successfully at t = 8.3s.

**5. Conclusion:** As an extended Kolmogorov system, the Yang chaotic system's mechanical and physical foundations are examined in this work. In order to find the main causes of chaos, we have combined four different forms of torques for the converted Yang chaotic system and examined five different scenarios. In the conservative cases, the Hamiltonian is constant, hence the analogous equation has a periodic solution. A conserved system's Hamiltonian tends to zero or infinity when an external or dissipative torque is applied, and chaos is avoided as a result. When all of the torques and the interchange of kinetic and potential energy are considered, the Yang system produces chaos. These four torques are necessary for the Yang system to become chaotic.

Moreover, FMPS for Yang chaotic system has been accomplished, and Fig.7. shows that the state trajectories of the error system approaches to zero after t = 8.3s. The efficiency of tactics and underlying theoretical analysis are validated by numerical simulations carried out in MATLAB. Despite the intricacy of this method, communication security is improved. The authors are sure that researchers in the fields of science and engineering would value this effort.

#### **References:**

- 1. Alvarez, G., Li, S., Montoya, F., Pastor, G. and Romera, M. (2005), Breaking projective chaos synchronization secure communication using filtering and generalized synchronization, *Chaos, Solitons and Fractals*, 24, 775-783.
- 2. Lorenz, E. N. (1963), Deterministic non-periods flows, Journal of the Atmospheric Sciences, 20, 130-141.
- 3. Chen, G. and Ueta, T. (1999), Yet another chaotic attractor, *International Journal of Bifurcation and Chaos*, 9(7), 1465-1466.
- 4. Pecora, L. M. and Carroll, T. L. (1990), Synchronization in chaotic systems, *Phys. Rev. Lett.*, 64 (8), 821-824.
- 5. Pecora, L. M. and Carroll, T. L. (1991), Driving systems with chaotic signals, *Physics Review Letter*, 44(4), 2374-2383.
- 6. Shukla, V. K., Joshi, M. C., Rajchakit, G., Nápoles Valdes, J. E., & Mishra, P. K. (2024). Matrix projective synchronization and mechanical analysis of unified chaotic system. Mathematical Methods in the Applied Sciences, 47(7), 6666-6682.
- 7. Gluhovsky, A. (2006), Energy-conserving and Hamiltonian low-order models in geo-physical fluid dynamics, *Nonlinear Process Geophys.*, 13(2), 125-133.

- 8. Pasini, A. and Pelino V. (2000), A unified view of Kolmogorov and Lorenz systems, *Phys. Lett. A*, 275, 435-446.
- 9. Shukla, V. K., Joshi, M. C., Mishra, P. K., & Xu, C. (2024). Mechanical analysis and function matrix projective synchronization of El-Nino chaotic system. *Physica Scripta*, *100*(1), 015255.
- 10. Shukla, V. K., Priyadarshi, A., Shukla, S., & Mishra, P. K. (2024). Study of Mechanical Analysis of Vallis Chaotic System. Journal of Applied Nonlinear Dynamics, 13(03), 449-459.
- 11. Mishra, P. K., and Das, S. (2016), Interaction between interfacial collinear Griffith cracks in composite media under thermal loading, *Zeitschrift für Naturforschung A*, 71(5), 465-473.
- 12. Mishra, P. K., Das, S., and Gupta, M. (2016), Interaction between interfacial and sub-interfacial cracks in a composite media-Revisited, *Journal of Applied Mathematics and Mechanics*, 96(9), 1129-1136.
- 13. Anuvedita Singh, P. K. Mishra and S. Das, Dynamic stress intensity factors of an interfacial crack in orthotropic elastic strips under impact loading conditions, Z. Angew. Math. Mech., Vol. 99(1), pp. 1-16, 2019. DOI: 10.1002/zamm.201800143.
- 14. Mishra, P. K., Singh, P., & Das, S. (2017). Study of thermo-elastic cruciform crack with unequal arms in an orthotropic elastic plane. ZAMM-Journal of Applied Mathematics and Mechanics/Zeitschrift für Angewandte Mathematik und Mechanik, 97(8), 886-894.
- 15. Mishra, P. K., Singh, P., & Das, S. (2017). Interaction of three interfacial cracks between an orthotropic half-plane bonded to a dissimilar orthotropic layer with punch. *Zeitschrift für Naturforschung A*, 72(11), 1021-1029.
- 16. Pelion, V., Maimone, F. and Pasini, A. (2014), Energy cycle for the Lorenz attractor, *Chaos Solit. Fract.*, 64, 67-77.
- 17. Qi, G. and Liang, X. (2016), Mechanical analysis of qi four-wing chaotic system, *Nonlinear Dyn.*. 86(2), 1095-1106.
- 18. Arnold V. I. (1991), Kolmogorov's Hydrodynamic attractors, *Proc. R. Soc. London*, A 434, 19-22.
- 19. Liang, X. and Qi, G. (2017), Mechanical analysis and energy cycle of Chen chaotic system, *Brazilian Journal* of Physics, 47(3), 288-294.
- 20. Benkouider, K., Sambas, A., Bonny, T., Al Nassan, W., Moghrabi, I. A., Sulaiman, I. M., ... and Mamat, M. (2024), A comprehensive study of the novel 4D hyperchaotic system with self-exited multistability and application in the voice encryption, *Scientific Reports*, 14(1), 12993.
- 21. Shukla, V. K., Joshi, M. C., Mishra, P. K., & Xu, C. (2024). Adaptive fixed-time difference synchronization for different classes of chaotic dynamical systems. Physica Scripta, 99(9), 095264.
- 22. Shukla, V. K., Joshi, M. C., Rajchakit, G., Chakrabarti, P., Jirawattanapanit, A., & Mishra, P. K. (2023). Study of generalized synchronization and anti-synchronization between different dimensional fractional-order chaotic systems with uncertainties. Differential Equations and Dynamical Systems, 1-15.

- 23. Ouannas, A. and Raghib, Abu-Saris (2016), On matrix projective synchronization and inverse matrix projective synchronization for different and identical dimensional discrete-time chaotic systems, Journal of Chaos, 2016, 1-7. http://dx.doi.org/10.1155/2016/4912520.
- 24. Shukla, V. K., Mishra, P. K., Srivastava, M., Singh, P., & Vishal, K. (2023). Matrix and Inverse Matrix Projective Synchronization of Chaotic and Hyperchaotic Systems with Uncertainties and External Disturbances. Discontinuity, Nonlinearity, and Complexity, 12(04), 775-788.
- 25. Shukla, V. K., Mbarki, L., Shukla, S., Vishal, K., & Mishra, P. K. (2023). Matrix projective synchronization between time delay chaotic systems with disturbances and nonlinearity. International Journal of Dynamics and Control, 11(4), 1926-1933.
- 26. Shukla, V. K., Joshi, M. C., Rajchakit, G., Nápoles Valdes, J. E., and Mishra, P. K. (2024). Matrix projective synchronization and mechanical analysis of unified chaotic system. Mathematical Methods in the Applied Sciences, 47(7), 6666-6682.
- 27. Liu, F. (2014), Matrix projective synchronization of chaotic systems and the application in secure communication, Applied mechanics and materials, 644, 4216-4220.
- 28. Wu, Z., Xu, X., Chen, G. and Fu, X. (2014), Generalized matrix projective synchronization of general colored networks with different-dimensional node dynamics, Journal of the Franklin Institute, 351, 4584-4595.
- 29. Shi, Y., Wang, X., Zeng, X. and Cao, Y. (2019), Function matrix projective synchronization of non-dissipatively coupled heterogeneous systems with different-dimensional nodes, Advances in Difference Equations, 198, 1-12, https://doi.org/10.1186/s13662-019-1984-9.
- 30. Petráš, I. (2022). The fractional-order Lorenz-type systems: A review. Fractional Calculus and Applied Analysis, 25(2), 362-377.

